Quantum Monte Carlo simulation of the one-dimensional spin-S xxz model. II. High precision calculations for S=1/2

1985 J. Phys. A: Math. Gen. 18 3189

(http://iopscience.iop.org/0305-4470/18/16/020)

J. Phys. A: Math. Gen. **18** (1985) 3189-3203. Printed in Great Britain

Quantum Monte Carlo simulation of the one-dimensional spin-S xxz model: II. High precision calculations for $S=\frac{1}{2}$

Mihail Marcu, Jürgen Müller and Franz-Karl Schmatzer

Fakultät für Physik, Universität Freiburg, Hermann-Herder-Strasse 3, D-7800 Freiburg, West Germany

Received 4 January 1985, in final form 22 March 1985

Abstract. A quantum Monte Carlo method developed in the first paper of this series is used to investigate the spin-$\frac{1}{2}$ isotropic ferromagnet and antiferromagnet. Critical indices are computed in a high precision simulation. We obtain $\alpha=-0.261\pm0.013$, $\gamma=1.552\pm0.008$ for the ferromagnet, and $\alpha=-1.202\pm0.009$, $\gamma=1.132\pm0.012$ for the antiferromagnet.

1. Introduction

In the first paper of this series (Marcu and Wiesler 1985, henceforth to be referred to as MW) we described a quantum Monte Carlo method for the xxz model defined by the Hamiltonian (throughout this paper we will use the notation of MW)

$$H=-\sum_{i=1}^{N}(S_i^xS_{i+1}^x+S_i^yS_{i+1}^y+J_zS_i^zS_{i+1}^z). \tag{1.1}$$

For a finite lattice size N, the quantum statistical expectation value $\langle A\rangle_N$ of the operator A is the $M\to\infty$ limit of the expectation value $\langle A_M\rangle_{N,M}$ computed in a classical two-dimensional model on an $N\times M$ chessboard lattice. This classical model is obtained via a path integral method that uses the Trotter formula (Trotter 1959, Suzuki 1976, Barma and Shastry 1978, MW). The couplings of the classical model vary with M, and the $M\to\infty$ limit is an infinite anisotropy limit. Note that for a finite M the operator A is in general also approximated by an operator A_M.

In order to compute the quantum statistical expectation values, two limits have to be performed. First, the $M\to\infty$ limit is done by using the fact that, for the quantities we are interested in

$$\langle A_M\rangle_{N,M}=\langle A\rangle_N+M^{-2}(\langle AB\rangle_N-\langle A\rangle_N\langle B\rangle_N)+O(M^{-3}) \tag{1.2}$$

(Schmatzer (1983), the technicalities of the $M\to\infty$ limit will be discussed in detail in a forthcoming publication). Here B is a sum over all lattice translations of some local operator. The coefficient of $1/M^2$ is certainly finite for any fixed value of N, and it is uniformly bounded as long as the model has a finite correlation length. Thus we have to compute $\langle A_M\rangle_{N,M}$ for a sequence of M and then, if M is high enough, do a linear fit in $1/M^2$. The second limit is the thermodynamic limit. It is implemented by choosing a lattice that is larger than the correlation length.

0305-4470/85/163189+15$02.25

In MW we discussed what quantities can be computed using our quantum Monte Carlo method. Besides thermodynamic quantities like mean energy and specific heat, we discussed the static structure function $I^{\alpha\alpha}(q)$ ($\alpha = x, y, z$), which is the thermodynamic limit of

$$I_N^{\alpha\alpha}(q) = Z_N^{-1} \operatorname{Tr} S^\alpha(q) S^\alpha(-q)\, \mathrm{e}^{-\beta H} \tag{1.3}$$

(β is the inverse temperature), with $S^\alpha(q)$ defined by

$$S^\alpha(q) = \frac{1}{\sqrt{N}} \sum_{r=1}^{N} \mathrm{e}^{-\mathrm{i}qr} S_r^\alpha, \qquad q = \frac{2\pi k}{N},\ k = 1, \ldots, N. \tag{1.4}$$

Here S_r^α are the generators of SU(2) at the lattice site r. On the $N \times M$ chessboard lattice $I_N^{zz}(q)$ is approximated by

$$I_{N,M}^{zz}(q) = \frac{1}{4NMZ_{N,M}} \sum_s \left(\sum_{j=1}^{M} s_j(q) s_j(-q) \right) \prod_{p=\text{even}} f(p) \tag{1.5}$$

where s is a spin configuration, $s = \{s_{rj}\colon r = 1, \ldots, N;\ j = 1, \ldots, M\}$, $s = \pm 1$, $f(p)$ are the plaquette weights defined in MW, $Z_{N,M}$ is the partition function, and $s_j(q)$ is defined by

$$s_j(q) = \sum_{r=1}^{N} \mathrm{e}^{-\mathrm{i}qr} s_{rj}, \qquad q = \frac{2\pi k}{N},\ k = 1, \ldots, N. \tag{1.6}$$

The static structure function is a quantity that can be measured in neutron scattering experiments on quasi-one-dimensional materials; it is proportional to the intensity of the scattered neutrons (Marshall and Lovesey 1971).

A quantity of great theoretical interest is the dynamic susceptibility $\chi^{\alpha\alpha}(q, \omega)$, which is proportional to the differential cross section in neutron scattering experiments. $\chi^{\alpha\alpha}(q, \omega)$ is defined by (t is the real time)

$$\chi^{\alpha\alpha}(q, \omega) = \tfrac{1}{4} \int_{-\infty}^{+\infty} \mathrm{d}t\, \mathrm{e}^{\mathrm{i}\omega t} \langle [S^\alpha(q, t), S^\alpha(-q, 0)] \rangle \tag{1.7}$$

where

$$S^\alpha(q, t) = \mathrm{e}^{\mathrm{i}Ht} S^\alpha(q)\, \mathrm{e}^{-\mathrm{i}Ht}. \tag{1.8}$$

Unfortunately we cannot compute $\chi^{\alpha\alpha}(q, \omega)$ in general with our Monte Carlo method. However, $\chi^{\alpha\alpha}(q, 0)$ (this corresponds to elastic neutron scattering) can be written as an integral over Euclidian time:

$$\chi^{\alpha\alpha}(q, 0) = \int_0^\beta \mathrm{d}\tau \langle S^\alpha(q, 0) S^\alpha(-q, \mathrm{i}\tau) \rangle. \tag{1.9}$$

On the $N \times M$ chessboard lattice $\chi^{zz}(q, 0)$ is approximated by

$$\chi_{N,M}^{zz}(q, 0) = \frac{\beta}{2NM^2 Z_{N,M}} \sum_s \left(\left| \sum_{j=\text{odd}} s_j(q) \right|^2 + \left| \sum_{j=\text{even}} s_j(q) \right|^2 \right) \prod_{p=\text{even}} f(p). \tag{1.10}$$

Note that in computing the quantum expectation value $\chi^{zz}(q, 0)$ for fixed N two approximations are made. Firstly, there is the usual approximation of the quantum expectation values by expectation values in the classical model on the $N \times M$ lattice. Secondly, the integral in (1.9) is approximated by a sum. As $M \to \infty$ the main correction term is in both cases proportional to $1/M^2$.

Since in this paper we are only dealing with the isotropic xxz model ($J_z = \pm 1$), we simplify our notation by writing $I(q)$ instead of $I^{zz}(q)$ and $\chi(q, 0)$ instead of $\chi^{zz}(q, 0)$.

The xxz spin-$\frac{1}{2}$ model at finite temperatures was also studied by de Raedt and Lagendijk (see the review paper by de Raedt and Lagendijk 1985). However, they do not have a procedure to carry out the $M \to \infty$ limit. Moreover, their method is restricted to $S = \frac{1}{2}$.

A $S = \frac{1}{2}$ quantum Monte Carlo method is also described by Hirsch *et al* (1982). The relation of their method to ours is discussed in MW.

One of the most interesting problems for spin-$\frac{1}{2}$ xxz chains is the critical behaviour in the isotropic ferromagnet and antiferromagnet cases. In order to investigate critical properties one must in fact carry out an additional limit, namely the $T \to 0$ limit (T is the temperature, the critical temperature being zero in one dimension). The computer time needed for our Monte Carlo simulation increases with decreasing temperature. The reason is twofold: both the values of M from which the higher order corrections in (1.2) become negligible, and the correlation length grow with decreasing temperature.

We performed a high accuracy calculation for the isotropic ferromagnet and antiferromagnet. In order to be able to reach low enough temperatures, we used the CRAY 1/M computer of Stuttgart University. The algorithm used was devised such as to make appropriate use of the vectorisation capabilities of the CRAY. It will be published elsewhere in a more general version, namely for the spin-S xyz model.

For the ferromagnet we obtained for the critical indices α and γ the values $\alpha = -0.261 \pm 0.013$, $\gamma = 1.552 \pm 0.008$. For the antiferromagnet we obtained $\alpha = -1.202 \pm 0.009$ and $\gamma = 1.132 \pm 0.011$.

These values for the critical indices do not agree with other values published for the ferromagnet. Lyklema (1983) used Handscomb's method (Handscomb 1962, 1964) to obtain $\alpha = -0.3 \pm 0.1$ and $\gamma = 1.75 \pm 0.02$. A similar calculation was done by Chakravarty and Stein (1982), but they did not consider temperatures low enough for the onset of the critical behaviour. The Handscomb method uses an expansion of $\exp(-\beta H)$ in powers of β. The discepancy between the Lyklema results and our should be resolved in the near future. Bonner and Fisher (1964) diagonalised the Hamiltonian exactly for small values of N and then extrapolated the results to the thermodynamic limit using an empirical numerical procedure. They obtained $\alpha = -0.475 \pm 0.025$ and $\gamma = 1.8$. For low temperatures, however, the correlation length is much larger than their values of N, and it is conceivable that their thermodynamic limit is not correct. Baker *et al* (1964) used a high temperature expansion supplemented by a Padé analysis to obtain $\gamma = 1.67 \pm 0.1$.

In our method, as opposed to the other methods discussed above, all steps in the calculation are under control. The only point of uncertainty remaining is the possibility that for temperatures lower than those considered here, the system crosses over to a different critical behaviour.

In § 2 we present our results for the isotropic ferromagnet and in § 3 those for the antiferromagnet. Our conclusions are given in § 4.

2. High precision simulation of the isotropic ferromagnet

As described in the introduction, our quantum Monte Carlo method involves taking two limits, namely the $M \to \infty$ limit and the thermodynamic limit.

Let us discuss the two limits in reverse order and start with the thermodynamic limit. This limit is performed by taking lattices with the value of $N/2$ larger than the correlation length (we take $N/2$ and not N because of the periodic boundary conditions). In practice the correlation length ξ is the value of r for which the correlation function $c(r)=\langle S_i^z S_{i+r}^z\rangle$ becomes zero within statistical errors. The first step in the quantum Monte Carlo method consists in running low precision simulations for several values of β in order to determine the values of N that will be used in the high precision simulation. The values of β and $N/2$ used in the high precision simulations are given in table 1 together with the correlation length estimated from these simulations.

Table 1. The values of β, ξ and $N/2$ for the ferromagnet.

β	1.0	1.65	2.7	3.5	4.5	5.75	7.4	9.5	12.2	15.65	20.0
ξ	5	7	9	11	11	14	18	20	21	26	28
$N/2$	10	10	12	16	16	20	20	28	28	40	46

For a fixed value of N, the $M\to\infty$ limit is performed by taking M high enough such that the behaviour of $\langle A\rangle_N-\langle A_M\rangle_{N,M}$ (see (1.2)) is linear in $1/M^2$. The value of M where the linear region is reached varies according to the quantity A considered. In table 2 we illustrate this point for the energy density e and the magnetic susceptibility $\chi(0,0)$. $M_{\min}$ is the numerical estimate of the value of M where the linear regime sets in. Since we do not consider all possible values of M, $M_{\min}$ should be viewed as a rough estimate. $M_{\max}$ is the highest value of M we consider.

Table 2. The values $M_{\min}$ and $M_{\max}$ for the energy density e and the susceptibility $\chi(0,0)$ (ferromagnet).

	Energy		Susceptibility	
β	$M_{\min}$	$M_{\max}$	$M_{\min}$	$M_{\max}$
15.65	24	38	10	38
12.20	16	36	10	36
9.50	14	34	10	34
7.40	12	32	6	32
5.75	10	30	6	30
4.50	8	26	4	26
3.50	6	26	4	26
2.70	4	26	4	26
1.65	2	18	2	26
1.00	2	16	2	14

In order to determine critical exponents, the physical quantities have to be measured with high accuracy. It turns out that we have to increase the number of sweeps both with increasing values of β and with increasing values of M. Moreover, for fixed values of the ratio β/M the number of sweeps has to be increased for increasing values of β. This situation is true both for the ferromagnet and for the antiferromagnet.

For the ferromagnet we also encountered another numerical problem. In the Monte Carlo simulation the successive measurements of a given quantity form a time series (Anderson 1971). In the ferromagnet case the time series correlation length increases sharply with increasing values of β and M (we used the group variance method for analysing the time series). For the antiferromagnet this does not happen.

This can be understood within the particle line picture of MW. For the ferromagnet, typical configurations contain clusters of particle lines, and plaquettes inside such a cluster cannot be changed by the local Monte Carlo procedure (see MW for details). For the antiferromagnet, typical configurations contain $N/2$ particle lines at a distance of two lattice spacings from one another. Therefore, many plaquettes are subject to updating by the local Monte Carlo procedure.

In table 3 we illustrate the numerical problems encountered in the Monte Carlo simulation of the ferromagnet. For three values of β we list the values of M used, the number of sweeps and, for the energy density and the susceptibility, the lower and higher estimates $\xi_{\min}$ and $\xi_{\max}$ of the correlation length of the time series together with the statistical errors. Although these estimates are rough, they reproduce the overall trend accurately. The different behaviour of the energy density and susceptibility clearly shows that one has to do the whole numerical analysis for each quantity separately. The quantity with the longest time series correlation is the susceptibility. This is to be expected since the susceptibility is unaffected by the local bending of particle lines described in MW.

Table 3. The values of N and M, the number N_s of sweeps, the lower and upper estimates for the time series correlation length ξ and the statistical errors (for both e and $\chi(0,0)$)—all listed for three values of β (ferromagnet).

				Energy			Susceptibility		
β	N	M	N_s	$\xi_{\min}$	$\xi_{\max}$	Δe	$\xi_{\min}$	$\xi_{\max}$	$\Delta\chi(0,0)$
1.0	20	2	20 000	1	10	0.000 31	1	1	0.005
	20	4	20 000	1	10	0.000 67	1	50	0.005
	20	6	20 000	40	40	0.001 1	40	80	0.006
	20	8	20 000	60	140	0.001 5	1	40	0.005
	20	10	20 000	60	60	0.001 9	1	40	0.005
	20	14	40 000	140	200	0.001 6	1	40	0.003
7.4	40	6	160 000	50	65	0.000 021	70	85	0.049
	40	8	160 000	70	90	0.000 041	70	90	0.067
	40	10	160 000	35	50	0.000 055	130	180	0.084
	40	12	160 000	70	70	0.000 075	90	110	0.10
	40	14	160 000	90	100	0.000 090	190	220	0.12
	40	18	160 000	40	90	0.000 11	190	240	0.12
	40	26	347 500	90	150	0.000 11	140	160	0.11
	40	32	430 000	120	120	0.000 11	120	210	0.10
15.65	80	10	500 000	10	200	0.000 0053	1	5	0.23
	80	12	500 000	500	800	0.000 0097	300	330	0.33
	80	14	1200 000	280	450	0.000 0089	500	800	0.26
	80	16	1000 000	1400	1400	0.000 014	1400	1650	0.42
	80	20	2000 000	500	1100	0.000 014	1400	1400	0.37
	80	24	2225 000	1400	1600	0.000 018	2000	2200	0.45
	80	30	3037 500	2200	2500	0.000 021	2500	3500	0.50
	80	38	3950 000	2500	3400	0.000 023	4500	5200	0.56

For $\beta = 20$ we did not take values of M high enough to determine the energy density, because this would have required an inordinate amount of computer time. Currently we are working on a computer program based on a completely new algorithm which will allow us to reach even lower temperatures.

The *xxz* model is exactly soluble at zero temperature (des Cloizeaux and Gaudin 1966). At $T = 0$ the energy density takes the value $e_0 = -\frac{1}{4}$. For a finite value of N the ground state is an $(N+1)$-dimensional SU(2) multiplet. Using the Wigner-Eckart theorem, it is then straightforward to show that

$$\lim_{T\to 0} \langle S_i^z S_{i+r}^z \rangle = \tfrac{1}{12}$$

$$\lim_{T\to 0} I(q) = \tfrac{1}{6}(1 + 2\pi\delta(q)) \tag{2.1}$$

$$\lim_{T\to 0} \chi(q, 0) = 1/3(1 + \cos q), \qquad q \neq 0.$$

Let us now present our results. In table 4 we list the values of the energy density e, of $e - e_0$, of the statistical error Δe of e, and of the percentage error of $e - e_0$. These results allow for a determination of the critical exponent α, since

$$e - e_0 \sim \beta^{\alpha - 1}. \tag{2.2}$$

In figure 1 we give a log-log plot of $e - e_0$ against β together with a linear fit through the last four data points. The estimated critical exponent is $\alpha = -0.261 \pm 0.013$.

Table 4. Monte Carlo results for the ferromagnetic energy density e (% represents the percentage error of $e - e_0$).

β	e	$e - e_0$	Δe	%
15.65	−0.244 62	0.005 38	0.000 054	1.00
12.20	−0.242 59	0.007 41	0.000 051	0.69
9.50	−0.239 84	0.010 16	0.000 084	0.82
7.40	−0.236 16	0.013 84	0.000 132	0.95
5.75	−0.231 14	0.018 86	0.000 130	0.69
4.50	−0.224 85	0.025 15	0.000 160	0.64
3.50	−0.216 33	0.033 67	0.000 170	0.51
2.70	−0.205 69	0.044 32	0.000 390	0.89
1.65	−0.174 75	0.075 25	0.000 610	0.81
1.00	−0.133 36	0.116 64	0.000 890	0.76

The critical exponent α can also be computed from other physical quantities. For the ferromagnet, the specific heat results are not accurate enough to allow for a determination of α within reasonable errors. This is caused by the fact that α is quite small. The errors in the specific heat are around 4% (as opposed to MW, in this paper the errors are given at a confidence level of 68%, i.e. one standard deviation). Our specific heat results are consistent with Blöte (1975).

Equation (2.1) shows that the spatial correlation function $c(r)$ converges to $\frac{1}{12}$ as $T \to 0$ (for $r \neq 0$). For the ferromagnet $c(1)$ is directly related to the energy density e

$$c(1) = -\tfrac{1}{3}e. \tag{2.3}$$

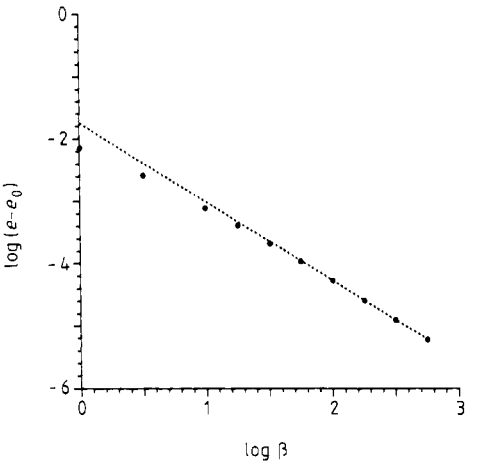

Figure 1. Logarithmic plot of the ferromagnetic energy density.

In table 5 we list our results for $c(1)$. They are not as accurate as the energy density results (for the antiferromagnet this is not true). From the last seven data points we extrapolate for α the value $\alpha = -0.218 \pm 0.038$.

Table 5. Monte Carlo results for $c(1)$ (ferromagnet).

β	$3c(1)$	$3\Delta c(1)$
12.20	0.242 73	0.001 16
9.50	0.240 48	0.001 38
7.40	0.236 01	0.001 14
5.75	0.231 76	0.000 73
4.50	0.225 13	0.000 91
3.50	0.216 77	0.000 65
2.70	0.203 73	0.001 53
1.65	0.172 98	0.001 41
1.00	0.134 05	0.001 33

The magnetic susceptibility $\chi(0, 0)$ diverges as $T \to 0$. In table 6 we list the values of $\chi(0, 0)$, the corresponding statistical errors $\Delta\chi(0, 0)$ and the percentage errors. Using these results we can determine the critical exponent γ:

$$\chi(0, 0) \sim \beta^{\gamma}. \tag{2.4}$$

Figure 2 shows a log-log plot of $\chi(0, 0)$ against β, together with a linear fit through the last seven data points. The extrapolated value for γ is $\gamma = 1.552 \pm 0.008$.

In figure 3 we plot our results for the static structure function $I(q)$, in figure 4 we plot the dynamic susceptibility $\chi(q, 0)$. Both converge towards the $T \to 0$ limits of (2.1). The results for $I(q)$ and $\chi(q, 0)$ for some values of q are listed in table 7.

Table 6. Monte Carlo results for $\chi(0,0)$ (ferromagnet).

β	$\chi(0,0)$	$\Delta\chi(0,0)$	%
20.00	30.380	0.980 00	3.23
15.65	20.653	0.372 53	1.80
12.20	13.959	0.208 73	1.50
9.50	9.661	0.156 05	1.62
7.40	6.442	0.074 52	1.16
5.75	4.363	0.037 31	0.86
4.50	2.988	0.018 24	0.61
3.50	2.076	0.010 72	0.52
2.70	1.436	0.014 84	1.03
1.65	0.713	0.007 19	1.01
1.00	0.367	0.003 63	0.99

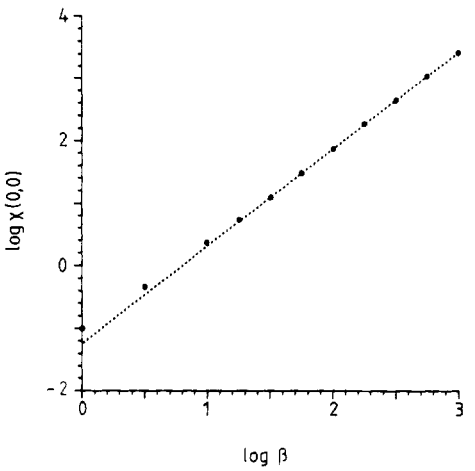

Figure 2. Logarithmic plot of the ferromagnetic susceptibility.

3. High precision simulation for the isotropic antiferromagnet

For the antiferromagnet the asymptotic $T \to 0$ behaviour sets on at a higher temperature than for the ferromagnet. In table 8 we list the values of β, $N/2$ and ξ used in our high precision simulation. At the same temperature, the correlation length is longer than for the ferromagnet.

In table 9 we list the values of $M_{\min}$ and $M_{\max}$ for the energy density e and the staggered susceptibility $\chi(\pi, 0)$. For the antiferromagnet it is $\chi(\pi, 0)$ rather than $\chi(0, 0)$ that diverges as $T \to 0$. From table 9 we see that for the antiferromagnet the linear region in $1/M^2$ is reached at higher values of M than for the ferromagnet.

In table 10 we list, for three values of β, the values of M used, the corresponding number of sweeps and the statistical errors of e and $\chi(\pi, 0)$. In the linear-in-$1/M^2$ regime, the errors of e show a slower increase with M than for the ferromagnet, and the errors of $\chi(\pi, 0)$ do not increase at all with M. Another difference from the ferromagnet is that the time series correlations stay short range even for large values of β or M, as mentioned in § 2.

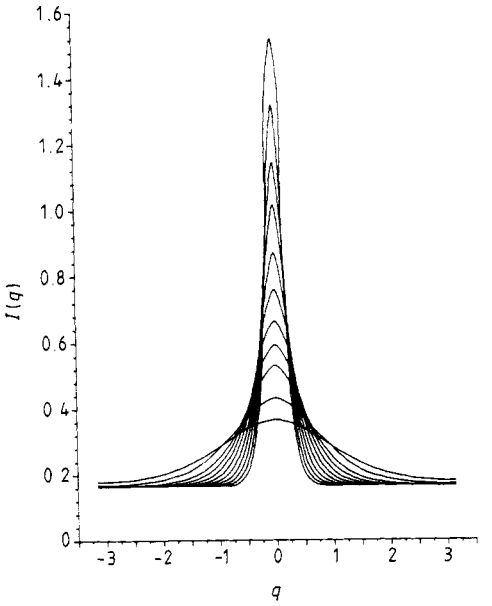

Figure 3. $I(q)$ for the ferromagnet. Some numerical values of $I(q)$ can be found in table 7. At the peak, the higher values of $I(0)$ correspond to the higher values of β.

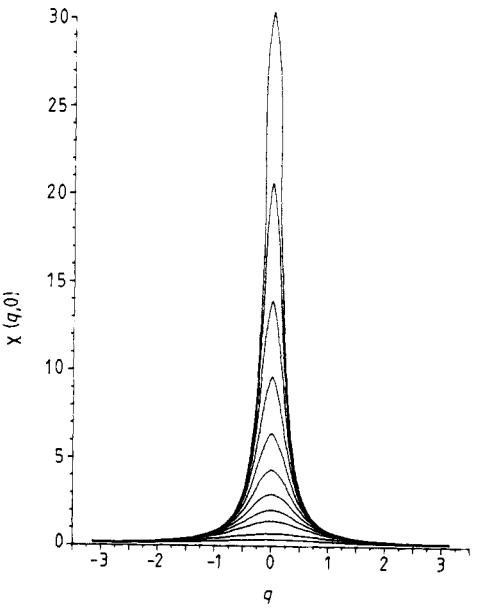

Figure 4. $\chi(q, 0)$ for the ferromagnet. Some numerical values of $\chi(q, 0)$ can be found in table 7. At the peak, the higher values of $\chi(0, 0)$ correspond to the higher values of β.

For the antiferromagnet, the critical exponent α can be determined from the energy density, from the specific heat and from $c(1)$. At $T=0$ the energy density takes the value $e_0=\frac{1}{4}-\log 2$. In table 11 we list the quantum Monte Carlo results for e, $e-e_0$,

Table 7. The values of $I(q)$ and $\chi(q,0)$ for some values of q for the ferromagnet. The integer $k=0,\ldots,N/2$ is defined by $q=2\pi k/N$. The numbers in brackets are the errors in the last two figures.

β	$\chi(\pi/2,0)$	$\chi(\pi,0)$	$I(0,0)$	$I(\pi/2,0)$	$I(\pi,0)$
20.00	0.3567 (31)	0.173 7 (15)	1.521 (46)	0.166 16 (63)	0.164 50 (61)
15.65	0.3702 (15)	0.175 48 (89)	1.319 (23)	0.166 77 (39)	0.166 43 (52)
12.20	0.3781 (15)	0.179 43 (81)	1.144 (17)	0.166 38 (41)	0.166 593 (40)
9.50	0.3883 (17)	0.185 7 (10)	1.017 (16)	0.166 27 (41)	0.166 27 (40)
7.40	0.3968 (18)	0.191 75 (96)	0.8711 (99)	0.167 05 (44)	0.166 41 (52)
5.75	0.3970 (14)	0.198 95 (79)	0.7589 (64)	0.168 05 (33)	0.165 87 (37)
4.50	0.3946 (13)	0.203 89 (92)	0.6640 (40)	0.171 04 (35)	0.165 32 (35)
3.50	0.3826 (10)	0.206 79 (80)	0.5930 (30)	0.177 73 (45)	0.165 09 (37)
2.70	0.3607 (23)	0.205 7 (19)	0.5319 (54)	0.187 37 (98)	0.166 22 (97)
1.65	0.2940 (21)	0.187 6 (19)	0.4320 (43)	0.207 7 (13)	0.169 2 (12)
1.00	0.2153 (14)	0.151 7 (16)	0.3668 (36)	0.229 4 (14)	0.178 9 (16)

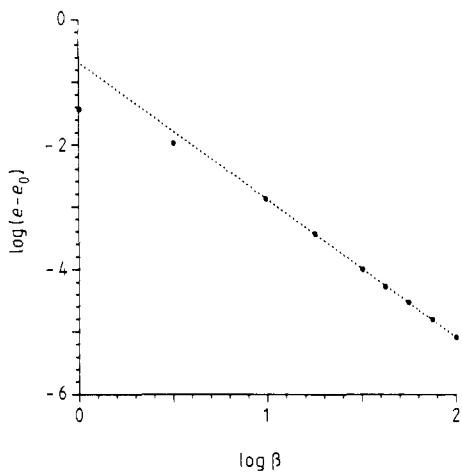

Figure 5. Logarithmic plot for the antiferromagnetic energy density.

Table 8. The values of β, ξ and $N/2$ for the antiferromagnet.

β	1.0	1.65	2.7	3.5	4.5	5.08	5.75	6.52	7.4
ξ	5	7	12	15	17	19	21	24	26
$N/2$	10	10	16	16	20	22	24	28	30

the error Δe, the specific heat C and the error ΔC. In table 12 we list the values of $3c(1)$, $3c(1)-e_0$, and the error $3\Delta c(1)$ (as opposed to the ferromagnet, $3c(1)=e$). Using the last seven data points for e, we extrapolate the value $\alpha=-1.202\pm0.009$, as seen from the log-log plot of figure 5. From the last seven data points for $c(1)$ we extrapolate the value $\alpha=-1.215\pm0.011$. The specific heat allows for a determination of α with a larger error. In figure 6 it is shown that an extrapolation through the last six data points yields the value $\alpha=-1.232\pm0.040$.

Table 9. The values M_{min} and M_{max} for the energy density e and staggered susceptibility $\chi(\pi, 0)$ (antiferromagnet).

	Energy		Susceptibility	
β	M_{min}	M_{max}	M_{min}	M_{max}
7.40	22	56	14	56
6.52	22	46	12	46
5.75	16	40	10	40
5.08	14	38	10	38
4.50	12	34	10	34
3.50	8	26	8	26
2.70	6	20	4	20
1.65	2	18	4	18
1.00	2	14	2	14

Table 10. The values of N and M, the number N_s of sweeps, and the statistical errors (for both e and $\chi(\pi, 0)$)—all listed for three values of β.

β	N	M	N_s	Δe	$\Delta\chi(\pi, 0)$
1.0	20	2	15 000	0.000 71	0.0057
	20	4	15 000	0.000 84	0.0047
	20	6	15 000	0.001 8	0.0048
	20	8	15 000	0.002 1	0.0048
	20	10	15 000	0.002 8	0.0045
	20	12	15 000	0.003 3	0.0045
	20	14	15 000	0.003 3	0.0048
3.5	32	4	140 000	0.000 16	0.023
	32	6	140 000	0.000 15	0.016
	32	8	140 000	0.000 17	0.013
	32	10	180 000	0.000 17	0.011
	32	12	180 000	0.000 19	0.011
	32	14	180 000	0.000 23	0.012
	32	16	200 000	0.000 22	0.013
	32	20	230 000	0.000 25	0.012
	32	26	260 000	0.000 27	0.012
7.4	60	8	450 000	0.000 050	0.054
	60	10	450 000	0.000 045	0.042
	60	12	450 000	0.000 044	0.037
	60	14	450 000	0.000 043	0.035
	60	16	570 000	0.000 043	0.029
	60	18	660 000	0.000 042	0.028
	60	22	780 000	0.000 044	0.027
	60	28	840 000	0.000 049	0.028
	60	36	840 000	0.000 058	0.030
	60	46	1050 000	0.000 061	0.029
	60	56	1500 000	0.000 060	0.028

The staggered susceptibility diverges as $T \to 0$. In table 13 we list the values of $\chi(\pi, 0)$ and the corresponding errors and the percentage errors. Using these results we extrapolate the value $\gamma = 1.132 \pm 0.011$ as shown in figure 7.

Table 11. Monte Carlo results for the antiferromagnetic energy density (% represents the percentage error of $e - e_0$) and specific heat.

β	e	$e - e_0$	Δe	%	C	ΔC
7.40	−0.436 98	0.006 17	0.000 075	1.22	0.1035	0.0051
6.52	−0.434 97	0.008 18	0.000 119	1.45	0.1190	0.0058
5.75	−0.432 37	0.010 77	0.000 129	1.20	0.1400	0.0058
5.08	−0.429 28	0.013 87	0.000 139	1.00	0.1619	0.0058
4.50	−0.424 78	0.018 37	0.000 171	0.93	0.1844	0.0059
3.50	−0.410 87	0.032 28	0.000 228	0.71	0.2580	0.0055
2.70	−0.386 77	0.056 38	0.000 453	0.80	0.2986	0.0130
1.65	−0.304 84	0.138 31	0.000 885	0.64	0.3367	0.0091
1.00	−0.204 64	0.238 51	0.001 244	0.52	0.1902	0.0028

Table 12. Monte Carlo results for $c(1)$ (antiferromagnet).

β	$3c(1)$	$3c(1) - e_0$	$3\Delta c(1)$
7.4	−0.436 86	0.006 28	0.000 127
6.52	−0.435 08	0.008 07	0.000 123
5.75	−0.432 47	0.010 68	0.000 164
5.08	−0.429 16	0.013 99	0.000 164
4.5	−0.425 03	0.018 12	0.000 196
3.5	−0.410 44	0.032 71	0.000 295
2.7	−0.386 44	0.056 70	0.000 541
1.65	−0.305 92	0.137 23	0.000 895
1.0	−0.204 68	0.238 46	0.001 004

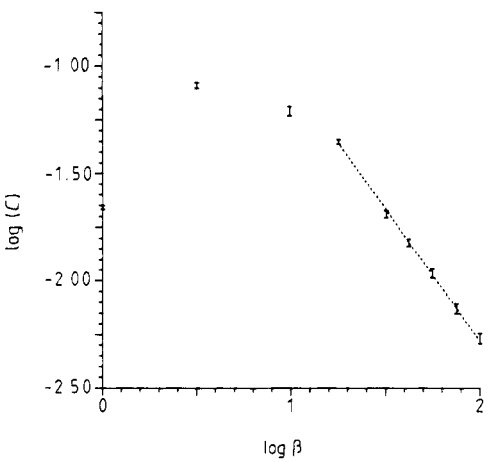

Figure 6. Logarithmic plot for the antiferromagnetic specific heat.

The quantity $I(\pi)$ also diverges as $T \to 0$. For the ferromagnet $I(0)$ is not independent from $\chi(0, 0)$, since $\chi(0, 0) = \beta I(0)$. For the antiferromagnet we are not aware of a similar relation between $\chi(\pi, 0)$ and $I(\pi)$. $I(\pi)$ diverges according to a power law of the type of (2.4) and we denote the corresponding exponent by $\bar{\gamma}$. In table 14 we

Table 13. Monte Carlo results for $\chi(\pi, 0)$ (antiferromagnet).

β	$\chi(\pi, 0)$	$\Delta\chi(\pi, 0)$	%
7.40	4.6247	0.024 33	0.56
6.52	4.0072	0.023 29	0.53
5.75	3.4606	0.020 82	0.60
5.08	3.0202	0.016 82	0.56
4.50	2.6180	0.013 40	0.62
3.50	1.9462	0.012 23	0.63
2.70	1.4170	0.011 41	0.80
1.65	0.7423	0.007 72	1.04
1.00	0.3814	0.003 22	0.84

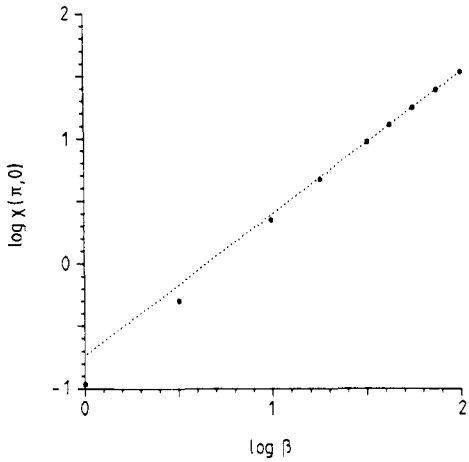

Figure 7. Logarithmic plot for the staggered antiferromagnetic susceptibility.

Table 14. Monte Carlo results for $I(\pi)$ (antiferromagnet).

β	$I(\pi)$	$\Delta I(\pi)$
7.40	1.0245	0.0034
6.52	0.9851	0.0035
5.75	0.9451	0.0036
5.08	0.9102	0.0033
4.50	0.8751	0.0036
3.50	0.7936	0.0034
2.70	0.7115	0.0042
1.65	0.5494	0.0046
1.00	0.4246	0.0032

list the values of $I(\pi)$ and the corresponding errors. A linear fit through the last five data points leads to the value $\bar{\gamma} = 0.317 \pm 0.007$.

In figure 8 we plot our results for $I(q)$ and in figure 9 we plot $\chi(q, 0)$. The numerical results for $I(q)$ and $\chi(q, 0)$ for some values of q are listed in table 15.

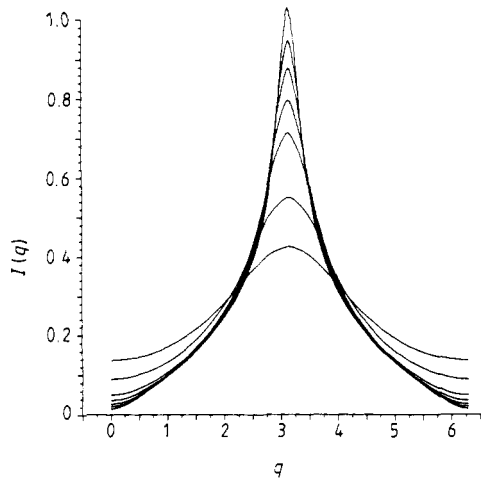

Figure 8. $I(q)$ for the antiferromagnet. Some numerical values of $I(q)$ can be found in table 15. At the peak, the higher values of $I(\pi)$ correspond to the higher values of β.

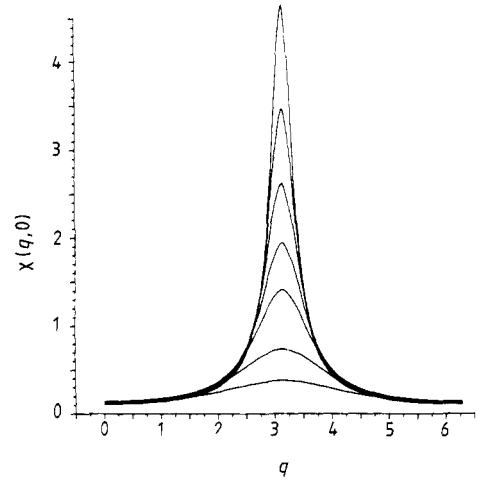

Figure 9. $\chi(q, 0)$ for the antiferromagnet. Some numerical values of $\chi(q, 0)$ can be found in table 15. At the peak, the higher values of $\chi(\pi, 0)$ correspond to the higher values of β.

4. Conclusions and outlook

For the first time a high precision quantum Monte Carlo simulation was performed. The results are accurate enough to investigate the critical behaviour of the *xxz* spin-$\frac{1}{2}$ ferromagnet and antiferromagnet.

At present we are continuing the investigation of the *xxz* models using generalisations of our method for higher spins on the one hand, and for spin-$\frac{1}{2}$ but more than one dimension on the other.

Table 15. The values of $I(q)$ and $\chi(q, 0)$ for some values of q for the antiferromagnet, presented in the same way as for the ferromagnet.

β	$\chi(\pi/2, 0)$	$\chi(0, 0)$	$I(\pi/2)$	$I(0)$
7.40	0.204 09 (31)	0.115 91 (38)	0.170 47 (14)	0.015 665 (52)
6.52	0.205 67 (45)	0.118 26 (42)	0.170 35 (18)	0.018 138 (63)
5.75	0.209 06 (49)	0.119 27 (41)	0.170 45 (18)	0.020 768 (83)
5.08	0.211 74 (44)	0.120 60 (38)	0.170 80 (21)	0.023 739 (74)
4.50	0.216 43 (56)	0.123 21 (30)	0.171 03 (18)	0.029 853 (68)
3.50	0.227 63 (62)	0.128 12 (47)	0.173 34 (34)	0.036 61 (13)
2.70	0.240 6 (13)	0.135 1 (10)	0.177 87 (70)	0.050 04 (37)
1.65	0.243 7 (16)	0.146 2 (10)	0.197 12 (80)	0.088 58 (65)
1.00	0.202 0 (12)	0.136 3 (11)	0.221 9 (15)	0.136 3 (11)

Acknowledgments

We would like to thank Professor Honerkamp for his constant support and advice during the completion of this work. One of us (MM) wishes to thank Dr K Fredenhagen for his constant interest and for many helpful discussions. Two of us (JM and FKS) are grateful to the Deutsche Forschungsgemeinschaft for financial support. We would also like to thank the computer centres of the Stuttgart and Freiburg Universities. Without their support this work could not have been done. Last but not least one of us (MM) would like to thank Mr Martin Walter for invaluable advice in the use of computer networks.

References

Anderson T W 1971 *The Statistical Analysis of Time Series* (New York: Wiley)
Baker G A, Rushbrooke G S and Gilbert H E 1964 *Phys. Rev.* **135** A1272
Barma M and Shastry B S 1978 *Phys. Rev.* B **18** 3351
Blöte H W J 1975 *Physica* **79B** 427
Bonner J C and Fisher M E 1969 *Phys. Rev.* **135** A640
Chakravarty S and Stein D B 1982 *Phys. Rev. Lett.* **49** 582
de Raedt H and Lagendijk A 1985 *Phys. Rep.* to be published
des Cloizeaux J and Gaudin M 1966 *J. Math. Phys.* 7 1384
Handscomb D C 1962 *Proc. Camb. Phil. Soc.* **58** 594
—— 1964 *Proc. Camb. Phil. Soc.* **60** 115
Hirsch J E, Sugar R L, Scalapino D J and Blankenbecler R 1982 *Phys. Rev.* B **26** 5033
Lyklema J W 1983 *Phys. Rev.* B **27** 3108
Marcu M and Wiesler A 1985 *J. Phys. A: Math. Gen.* **18** 2479
Marshall W and Lovesey S W 1971 *Theory of thermal neutron scattering* (Oxford: Clarendon)
Schmatzer F K 1983 *Diplomarbeit*
Suzuki M 1976 *Commun. Math. Phys.* **51** 183
Trotter H F 1959 *Proc. Am. Math. Soc.* **10** 545